Article

Assessment of the Response of Photosynthetic Activity of Mediterranean Evergreen Oaks to Enhanced Drought Stress and Recovery by Using PRI and R690/R630

Chao Zhang [1,2,*] (ID)**, Catherine Preece** [1,2]**, Iolanda Filella** [1,2]**, Gerard Farré-Armengol** [1,2] **and Josep Peñuelas** [1,2] (ID)

1   CSIC, Global Ecology Unit, CREAF-CSIC-UAB, Bellaterra, 08193 Barcelona, Catalonia, Spain;
     catherine.preece09@gmail.com (C.P.); iola@creaf.uab.cat (I.F.); g.farre@creaf.uab.cat (G.F.-A.);
     josep.penuelas@uab.cat (J.P.)
2   CREAF, Cerdanyola del Vallès, 08193 Barcelona, Catalonia, Spain
*   Correspondence: c.zhang@creaf.uab.cat; Tel.: +34935813355

Abstract: The photochemical reflectance index (PRI) and red-edge region of the spectrum are known to be sensitive to plant physiological processes, and through measurement of these optical signals it is possible to use non-invasive remote sensing to monitor the plant photosynthetic status in response to environmental stresses such as drought. We conducted a greenhouse experiment using *Quercus ilex*, a Mediterranean evergreen oak species, to investigate the links between leaf-level PRI and the red-edge based reflectance ratio (R690/R630) with CO_2 assimilation rates (A), and photochemical efficiency (F_V/F_M and Yield) in response to a gradient of mild to extreme drought treatments (nine progressively enhanced drought levels) and corresponding recovery. PRI and R690/R630 both decreased under enhanced drought stress, and had significant correlations with A, F_V/F_M and Yield. The differential values between recovery and drought treatments of PRI ($\Delta PRI_{recovery}$) and R690/R630 ($\Delta R690/R630_{recovery}$) increased with the enhanced drought levels, and significantly correlated with the increases of $\Delta A_{recovery}$, $\Delta F_V/F_{M recovery}$ and $\Delta Yield_{recovery}$. We concluded that both PRI and R690/R630 were not only sensitive to enhanced drought stresses, but also highly sensitive to photosynthetic recovery. Our study makes important progress for remotely monitoring the effect of drought and recovery on photosynthetic regulation using the simple physiological indices of PRI and R690/R630.

Keywords: chlorophyll fluorescence (ChlF); drought; Mediterranean; photochemical reflectance index (PRI); photosynthesis; R690/R630; recovery

1. Introduction

The increasing occurrence of drought in the Mediterranean region is widely reported [1–3] and during the last 20 years observations show that it has affected ecosystem functioning and structure [4,5], decreased plant growth [6] and primary production [7,8], and triggered vegetation mortality [9]. The increase of drought has also enhanced water scarcity [10], and elicited ecological damage [11] and crop failures [12]. Faced with these negative impacts, monitoring the timing of drought onset and the extent of the effects on vegetation ecosystems is being increasingly warranted.

Summer drought, one of the key constraints of Mediterranean ecosystems [4], elicits a water deficit in the leaf tissue that can down-regulate photosynthesis [13]. This reduction in photosynthesis for Mediterranean species such as *Quercus ilex* L. is generally caused by stomatal closure in response to drought stress [14–16]. *Quercus ilex* is a broadleaved evergreen tree or shrub that is widely distributed

from semi-arid to humid areas of the Mediterranean region [17]. The sclerophyllous characteristics of *Q. ilex* make it possible to reduce its transpiration and to withstand the effect of long summer drought events. *Quercus ilex* also has the ability to reactivate its photosynthetic machinery and increase photosynthesis rates when the soil water content (SWC) is high enough to again support water transport through the plant [18].

When plants suffer water stress, the reducing power from photosynthesis becomes excessive, but then the increases in zeaxanthin pigments from xanthophyll de-epoxidation can safely dissipate excessive energy and prevent the photosystems from potential damage by accumulating excitation energy [19,20]. The photochemical reflectance index (PRI) was originally defined based on changes in zeaxanthin at the wavelength of 531 nm to assess the efficiency of absorbed photosynthetic active radiation (APAR) for photosynthesis (light use efficiency; LUE) [21,22]. A great number of studies have found that PRI is able to track LUE changes at diurnal and seasonal scales from leaf to canopy to ecosystem levels [23–25], because apart from xanthophyll pigments, PRI was also associated with changes of carotenoid/chlorophyll ratios [26–29], which play a key role in long-term dynamics of photosynthesis [20,30]. Increasing attention has been focused on using PRI to detect the effect of environmental stress (e.g., intense irradiance, water shortage, nutrition deficit, and high and low temperature stresses) on photosynthetic changes [8,14,31–36].

The changes in photosynthesis are synchronously accompanied by the emission of chlorophyll *a* fluorescence (ChlF), which is regulated by the photochemical conversion and heat dissipation of excitation energy [37]. The contribution of the ChlF emission is only a small part of the total radiation reflected from vegetation, however, ChlF is highly sensitive to the variability of plant physiological processes in response to various environmental conditions, and can provide a direct approach to detect the functional status of photosynthetic machinery [38,39]. The range of the ChlF emission spectrum is from the red to near-infrared regions, with two peaks at around 690 and 740 nm [38]. The active ChlF, mainly obtained from a pulse-amplitude modulated (PAM) fluorometer, has been extensively used for monitoring foliar photosynthetic apparatus [40]. Recently, the passive ChlF (solar-induced fluorescence, SIF), derived from such methods as the Fraunhofer Line Depth technique or laser induction, has scaled up the measurements and the applications for detecting photosynthesis from leaf level to canopy, ecosystem and regional scales [31,41–44].

Some studies have illustrated that reflectance ratios such as R690/R600, R690/R630, R690/R655, and R740/R800 were sensitive to the changes of ChlF, because the ChlF signal is superimposed on the red-edge of leaf reflectance [38,45,46]. These reflectance ratios have been shown to track the changes in fluorescence, photochemical efficiency and carbon assimilation rates for healthy and stressed plants due to high co-variation of red-edge reflectance/absorption, pigment concentration, and leaf physiology [31,47–53].

Numerous studies had shown PRI is sensitive to water stress [33,49,54–56], but no studies have illustrated that PRI was sensitive enough to track recovery after drought stress, at least to the best of our knowledge. Few studies so far have either exploited the applicability of the reflectance ratios based on the red-edge region of the spectrum for detecting the photosynthetic response to water stress [31,48,49]. Only the study by Dobrowski et al. [31] monitored photosynthetic response to water stress and recovery with only a four-day-long experiment.

Along with the increasing occurrence of drought, it is important to find an easy, non-destructive and efficient method to monitor both the effect of drought on plant physiological and functional variability and the subsequent recovery of the photosynthetic machinery. This is particularly important for regions confronted with progressively more extreme summer droughts such as the Mediterranean basin. Based on the previous studies, PRI and reflectance ratio based on the red-edge region of the spectrum (R690/R630) are thus promising methods to test such photosynthetic responses. In this study, we conducted a two-month long greenhouse experiment using the typical Mediterranean species *Q. ilex* by exposing the plants to nine different progressive drought treatments through controlling the SWC, and then re-watering for five weeks to explore the levels of plant recovery. We simultaneously

measured foliar reflectance to obtain PRI and R690/R630, PAM ChlF to get maximum (F_V/F_M) and actual (Yield) photochemical efficiency of photosystem II (ΦPSII), and CO_2 assimilation rates (*A*). We hypothesized that both PRI and R690/R630 would be sensitive to the progressively increasing drought, and could therefore be used to monitor photosynthetic dynamics. We also hypothesized that both PRI and R690/R630 would detect the photosynthetic recovery after experiencing different levels of drought stresses.

2. Material and Methods

2.1. Experimental Design

Three-year-old *Quercus ilex* saplings of approximately 60 cm height were obtained in May 2015 (Forestal Catalana, Barcelona, Spain) and were re-potted in 3.5 litre pots, with a substrate consisting of 45% sand, 45% autoclaved peat, and 10% natural soil inoculum. The soil was collected from a natural holm oak forest on a south-facing slope (25% slope) in the Prades Mountains in Northeastern Spain (41°13' N, 0°55' E). There were 162 saplings in total, divided into six blocks, and plants were grown in the greenhouse of the Autonomous University of Barcelona (Barcelona, Spain) with a six-week period of adequate watering, to allow them to acclimate to greenhouse conditions. During the experiment, in the greenhouse the mean air temperature was 26.7 °C (measured with EL-USB-2 data logger, Lascar Electronics, Wiltshire, UK), and the soil temperature monitored at a fine scale in five pots across the different soil types was 27.0 °C on average (measured with Decagon Em50 data logger with 5TM soil probes, Decagon Devices, Pullman, WA, USA). The saplings were then exposed to water stress by withholding water for nine different drought treatments with 18 plants each. The length of time without water ranged from 0 to 21 days, which means the first drought level, with 0-day withholding water, was effectively the control treatment. At the end of each treatment, the foliar photochemical efficiency of photosystem II (ΦPSII) and the reflectance were synchronously measured on half of the pots (nine per drought level) inside the greenhouse under clear skies within one hour of solar noon (12:00 to 14:00). The remaining pots then had six weeks of recovery, which involved re-watering at optimal levels, and then identical leaf measurements were collected for these plants.

The water content of the substrate was determined in each pot at the start of the study and at the end of its drought period, and recovery period, if relevant (using ML3 Theta Probe connected to a HH2 Moisture Meter from Delta-T Devices, Cambridge, UK). Mean soil moisture at the start of the experiment was 22.6% and it decreased exponentially to 0.3% at the end of the most extreme drought treatment. Soil moisture recovered quickly to ca. 20% within one week of re-watering and was 24.7% on average during the recovery phase. The differential SWC (ΔSWC$_{recovery}$) was calculated by subtracting the nine different drought treatments values from corresponding recovery treatments.

2.2. Leaf Photosynthesis Measurements

In the greenhouse, the CO_2 assimilation rates (*A*) of leaves were measured using an ADC pro (LCpro1Portable Photosynthesis System; ADC BioScientific Ltd., Hoddesdon, Herts, UK) gas exchange system. The measurements were conducted under a quantum flux density of 1000 µmol m^{-2} s^{-1} and ambient CO_2 concentration of 395 µmol mol^{-1}. Five measurements were recorded after the values were stabilized and had reached a steady state for each plant. After each measurement, the leaf area that was enclosed in the cuvette was marked on the leaves; leaves were later photographed and the leaf areas for which *A* was measured were estimated using ImageJ 1.46r (NIH, Bethesda, MD, USA) to standardize all *A* measurements. The differential *A* ($\Delta A_{recovery}$) was calculated by subtracting the nine different drought treatments values from corresponding recovery treatments.

2.3. Chlorophyll Fluorescence Measurements

Chlorophyll fluorescence measurements were performed by a pulse-amplitude-modulated photosynthesis yield analyzer (PAM-2000; Walz, Effeltrich, Germany). The measurements were

conducted on three healthy and mature leaves at the top of each plant. A saturating light pulse (SP) was applied to dark-adapted (at least 20 min) leaves for the determination of minimum (F_o) and maximum (F_M) fluorescence. The maximum photochemical efficiency of photosystem II (PSII) (F_V/F_M) was then calculated according to Genty et al. [57]:

$$F_V/F_M = (F_M - F_o)/F_M \tag{1}$$

In parallel with F_V/F_M, the actual photochemical efficiency of PSII (Yield) was also calculated based on the rapid measurements of steady-state (F_S) and the maximal (F_M') fluorescence yield during the full closing of the PSII center in light-adapted leaves under ambient light and full sun conditions around noon:

$$\text{Yield} = (F_M' - F_S)/F_M' \tag{2}$$

The differential F_V/F_M ($\Delta F_V/F_{Mrecovery}$) and Yield ($\Delta \text{Yield}_{recovery}$) between the nine different drought treatments values and recovery treatments were also calculated.

2.4. Reflectance Measurements

Leaf spectral reflectance measurements were collected using a broad range mini spectroradiometer (LR1; ASEQ, Vancouver, BC, Canada) with a fiber-optic of 25° field of view. The instrument measures spectral reflectance between 300 and 1000 nm with a sampling interval of less than 1 nm. To reduce atmospheric condition changes, the spectroradiometer was calibrated using a white Spectralon reference panel (Labsphere, North Sutton, NH, USA), which can be regarded as a Lambertian reflector. Incident solar irradiance was immediately determined using the same white reference panel prior to the radiance measurements. All spectral measurements were carried out at a nadir view angle ca. 1 cm above the leaf. The ground-projected instantaneous field of view (GIFOV) was thus about 4.4 mm. In each plant, we measured three different leaves at the top of the canopy as replicates. The photochemical reflectance index (PRI, [21,22]) was calculated from the reflectance data (Rx implies reflectance at x nm) as:

$$\text{PRI} = (R531 - R570)/(R531 + R570) \tag{3}$$

Additionally, we also retrieved the reflectance ratio R690/R630 based on the red-edge region of the spectrum. Because changes in the reflectance at 690 nm (R690) can be attributed to the absorptions of pigments, plant physiological variations and also ChlF which are associated with photosynthetic activity, and R630 is relatively less sensitive to photosynthesis and fluorescence emission [49].

The differential PRI ($\Delta \text{PRI}_{recovery}$) and R690/R630 ($\Delta R690/R630_{recovery}$) were obtained through nine different drought treatments values subtracted from corresponding recovery treatments.

2.5. Statistical Analysis

Differences of soil water content, CO_2 assimilation rate, photochemical efficiency of photosystem II (ΦPSII) and reflectance indices between the nine drought levels and corresponding plant recovery were analyzed using repeated-measures analyses of variance (ANOVAs). The differences were considered statistically significant at $p < 0.05$. The applicability of PRI and R690/R630 for assessing CO_2 assimilation, ΦPSII responses to drought stress and recovery were analyzed using standardized major-axis regression to identify correlations between the variables. All analyses were conducted with R version 3.3.2 (R Core Development Team, Vienna, Austria, 2016).

3. Results

3.1. Responses to Enhanced Drought Stress

In our experiment, the *Q. ilex* seedlings were treated by withholding watering from 0 to 21 days in nine different drought levels treatments. Along with the increasing days of drought and decreasing

soil water content (i.e., enhanced drought stress), CO_2 assimilation rates (A) and maximum (F_V/F_M) and actual (Yield) photosystem II efficiency (ΦPSII) decreased from highest values at the beginning of the experiment to lowest values in severe drought conditions (Figure 1). The physiological indices of the photochemical reflectance index (PRI) (Figure 1a) and reflectance ratio (R690/R630) (Figure 1b) also decreased gradually. Both changes in PRI and R690/R630 were highly consistent with the decreases in soil water content (SWC), A, F_V/F_M and Yield. However, in the last three extreme drought level treatments, PRI did not change significantly.
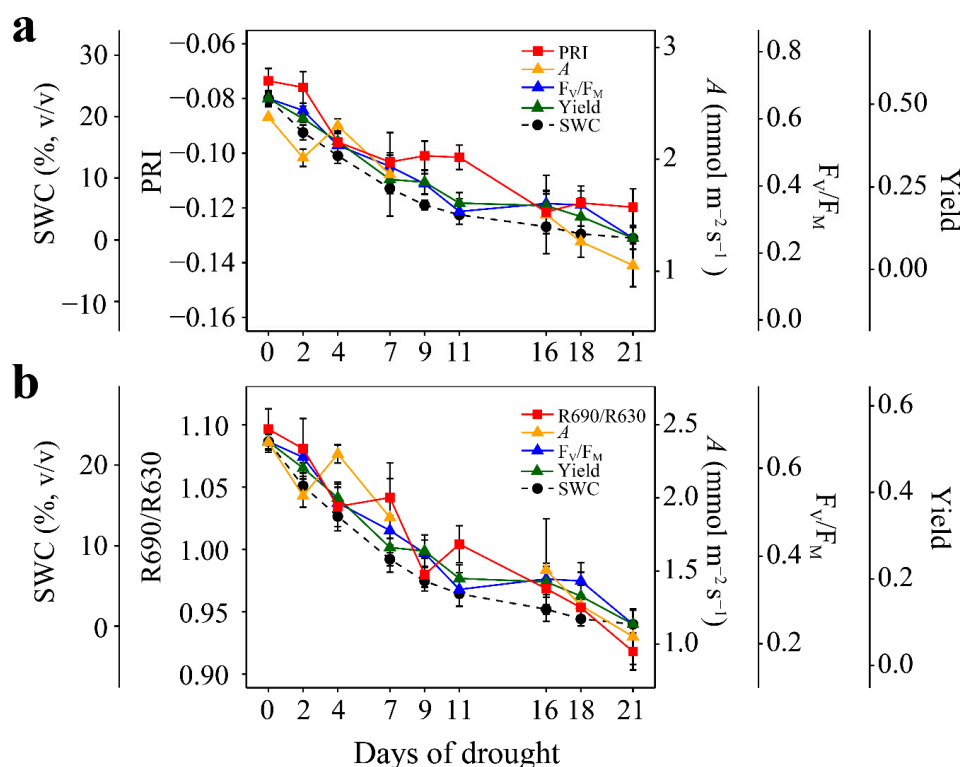

Figure 1. Changes in CO_2 assimilation rates (A), maximum (F_V/F_M) and actual (Yield) photochemical efficiency of photosystem II (ΦPSII), and soil water content (SWC) with the photochemical reflectance index (PRI) (**a**) and with reflectance ratio R690/R630 based on the red-edge region of the spectrum (**b**) in response to nine different drought levels treatment for *Quercus ilex*. Error bars denote the standard errors of the mean (n = 9).

3.2. Relationships of PRI and R690/R630 with A, F_V/F_M, and Yield under Enhanced Drought Stress

PRI and R690/R630 were used to assess the photosynthetic response to drought stress. Both PRI (Figure 2a) and R690/R630 (Figure 2b) were significantly correlated with A and explained 82% and 86% of variance of A, respectively. PRI had strong relationships with F_V/F_M and Yield ($R^2 \geq 0.85$ and $p < 0.001$ for both, Figure 2c). Similar significant correlations were found between R690/R630 and F_V/F_M and Yield ($R^2 = 0.89$ and $p < 0.001$ for both, Figure 2d). In contrast, the normalized difference vegetation index (NDVI, calculated by (R900 − R680)/(R900 + R680)) showed no significant correlation with A under enhanced drought conditions ($R^2 = 0.08$ and $p = 0.58$).
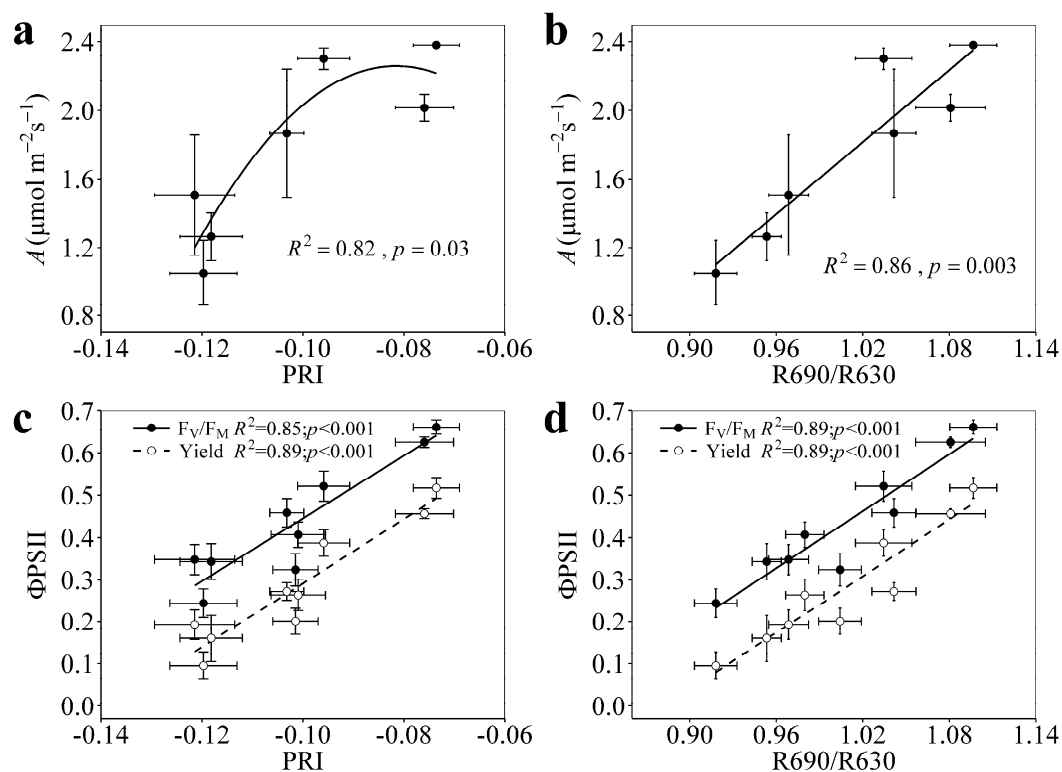
Figure 2. Relationships of *A* with PRI (**a**) and R690/R630 (**b**), and photochemical efficiency of PSII (ΦPSII) (F_V/F_M and Yield) with PRI (**c**) and R690/R630 (**d**) for *Quercus ilex*. All the values are from Figure 1.

3.3. Responses to Recovery

The SWC (Figure 3a) clearly recovered to the pre-drought (0-day drought level, namely, control treatment) condition in all drought treatments after five weeks of re-watering. They all reached identically high values, significantly higher than in the drought treatments from the 4-day drought level treatment onwards ($p < 0.001$). *A* (Figure 3b) was higher and remained similar in the recovery treatment, particularly in the last three severe drought treatments. The mean of F_V/F_M (Figure 3c) in the recovery treatment was significantly increased from the 7-day drought level treatment ($p < 0.001$). Yield (Figure 3d) presented analogous changes with SWC, *A*, and F_V/F_M and increased from the 9-day drought level treatment ($p < 0.001$). Both PRI (Figure 3e) and R690/R630 (Figure 3f) had no significant difference in the first four drought treatments with corresponding recovery treatments, but significantly increased from the recovery treatment of the 9-day drought level.

The differential values of variables were calculated by subtracting nine drought levels treatments from corresponding recovery treatments to assess the changes of photosynthesis after one month of re-watering the plants of the drought treatment, and to evaluate the applicability of PRI and R690/R630 in detecting the recovery. The values of $\Delta A_{recovery}$, $\Delta F_V/F_{Mrecovery}$, and $\Delta Yield_{recovery}$ increased in conjunction with increasing ΔSWC and increasing drought levels (Figure 4). Both $\Delta F_V/F_{Mrecovery}$ and $\Delta Yield_{recovery}$ increased slowly in the last three drought levels. Changes in $\Delta PRI_{recovery}$ (Figure 4a) were consistent with $\Delta A_{recovery}$, $\Delta F_V/F_{Mrecovery}$, and $\Delta Yield_{recovery}$. $\Delta R690/R630_{recovery}$ (Figure 4b) also showed a gradual increase as with the other variables, with a high value in the 9-day drought level treatment.
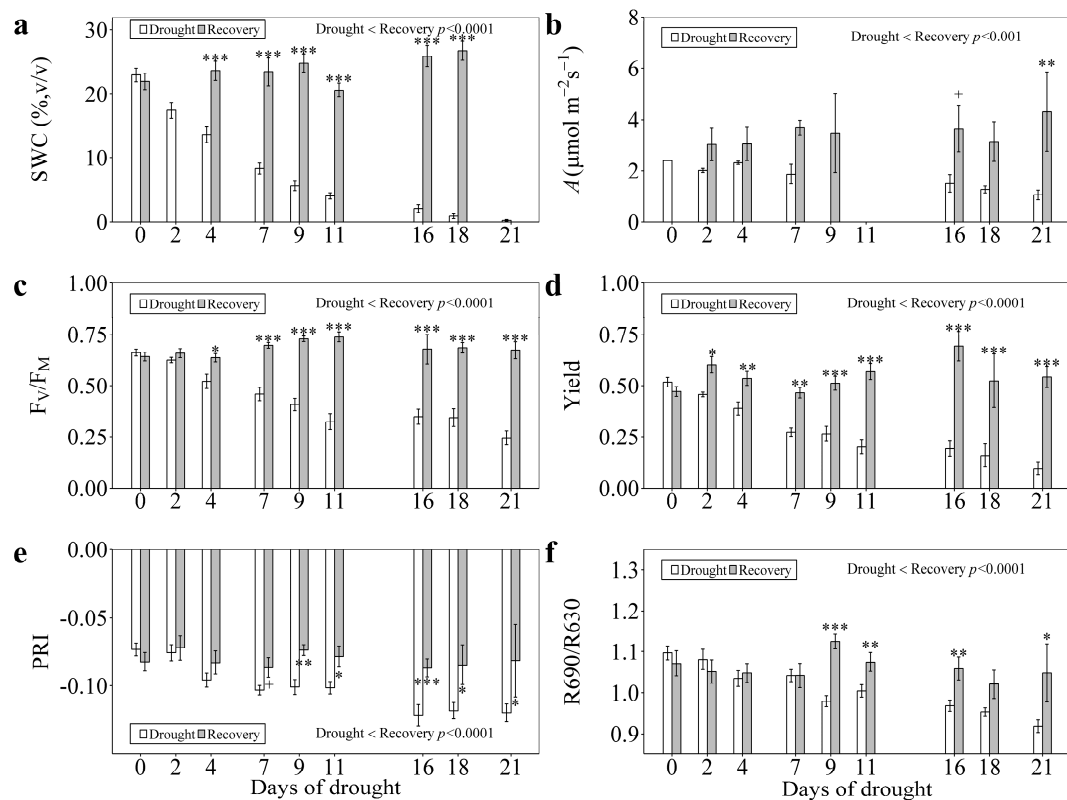
Figure 3. Changes in SWC (**a**), *A* (**b**), F_V/F_M (**c**), Yield (**d**), PRI (**e**) and R690/R630 (**f**) in response to nine different drought levels and corresponding recovery treatments for *Quercus ilex*. The significances were denoted as [+] $p < 0.1$, * $p < 0.05$, ** $p < 0.01$ and *** $p < 0.001$.
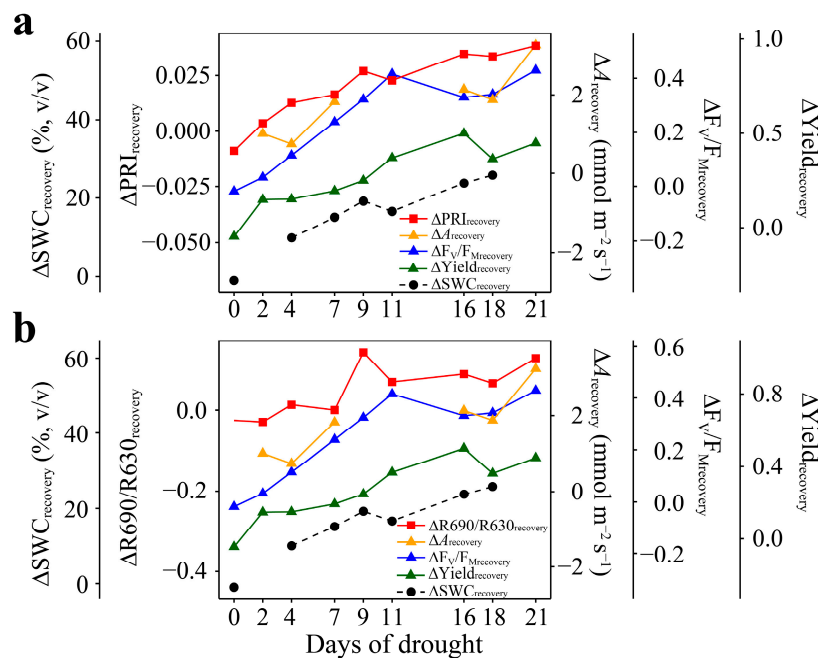

Figure 4. Changes in differential *A* (Δ*A*), $\Delta F_V/F_M$, ΔYield, and ΔSWC with ΔPRI (**a**) and with ΔR690/R630 (**b**) in response to nine different drought levels for *Quercus ilex*. The differential values of variables calculated by subtracting the mean of nine drought levels treatment from corresponding mean of recovery treatments in Figure 3.

3.4. Relationships of $\Delta PRI_{recovery}$ and $\Delta R690/R630_{recovery}$ with $\Delta A_{recovery}$, $\Delta F_V/F_{Mrecovery}$, and $\Delta Yield_{recovery}$

Both $\Delta PRI_{recovery}$ and $\Delta R690/R630_{recovery}$ accounted for large proportions of the variability of $\Delta A_{recovery}$ ($R^2 \geq 0.70$ and $p < 0.05$ for both, Figure 5a,b). $\Delta PRI_{recovery}$ was highly significantly correlated with $\Delta F_V/F_{Mrecovery}$ and $\Delta Yield_{recovery}$ ($R^2 \geq 0.85$ and $p < 0.001$ for both, Figure 5c). The relationships of $\Delta R690/R630_{recovery}$ with $\Delta F_V/F_{Mrecovery}$ and $\Delta Yield_{recovery}$ were also significant, but they were not as good as those of $\Delta PRI_{recovery}$ with $\Delta F_V/F_{Mrecovery}$ and $\Delta Yield_{recovery}$ (Figure 5d).
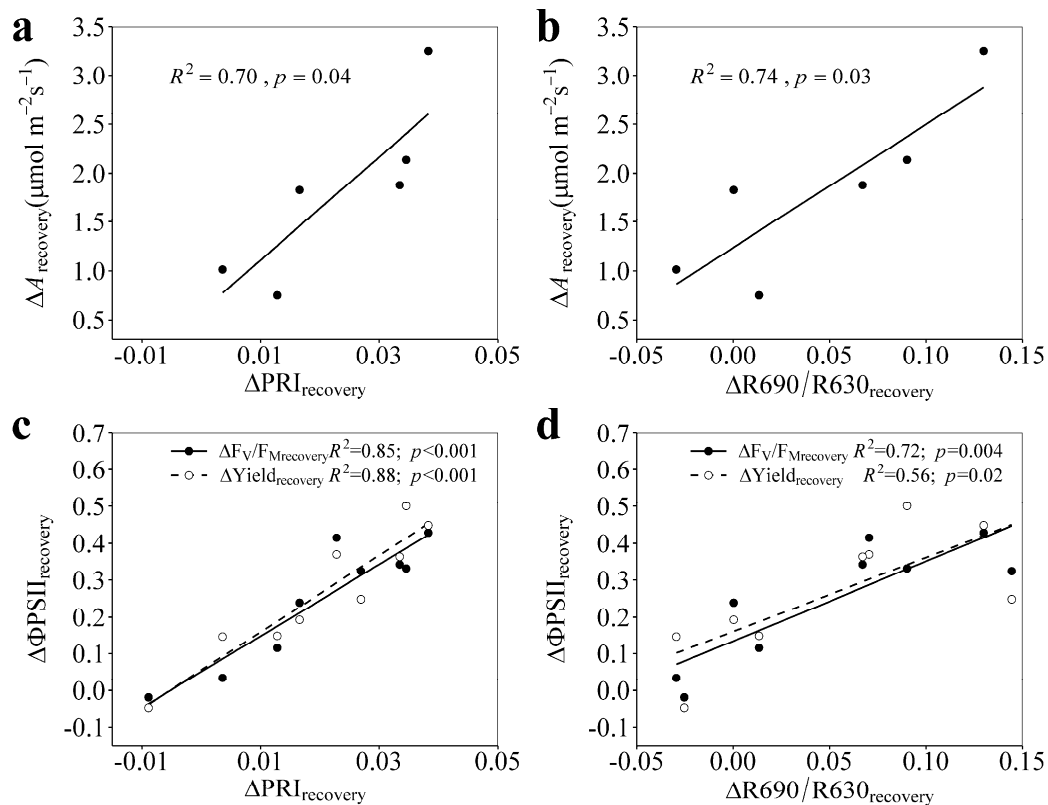

Figure 5. Relationships of differential A ($\Delta A_{recovery}$) with $\Delta PRI_{recovery}$ (**a**) and $\Delta R690/R630_{recovery}$ (**b**), and photochemical efficiency of PSII ($\Delta \Phi PSII$) (F_V/F_M and Yield) with $\Delta PRI_{recovery}$ (**c**) and $\Delta R690/R630_{recovery}$ (**d**) for *Quercus ilex*. All the differential values are from Figure 4.

4. Discussion

4.1. PRI and R690/R630 Tracked the Photosynthetic Changes under Enhanced Drought Levels

The enhanced levels of drought caused reductions in CO_2 assimilation rates (A) and photochemical efficiency of photosystem II ($\Phi PSII$) (F_V/F_M and Yield) in Mediterranean evergreen leaves (Figure 1). Similar trends were also recorded for the photochemical reflectance index (PRI, Figure 1a) and reflectance ratio based on the red-edge region of the spectrum (R690/R630, Figure 1b), indicating the sensitivity of PRI and R690/R630 to gradually increased drought stress. The close correspondence of PRI and R690/R630 with photosynthetic activity (Figure 3a) and $\Phi PSII$ (Figure 3b) demonstrated the promise of pigment- or red-edge reflectance-based approaches to remote monitoring of evergreen photosynthetic activity under gradually enhanced drought.

PRI is used to reveal the facultative xanthophyll cycle activity at short-term scale (hours to few days) [21,22,28], but also to estimate the changes in the constitutive pigment pool size at long-term scale (weeks to months) [27,29,58,59]. In our study, PRI showed promise as an index of photosynthetic down-regulation and illustrated the activation of photo-protective carotenoid pigments under photosynthetic down-regulation in response to gradually enhanced drought stress. During the summer

drying period, leaves in evergreen vegetation of semi-arid Mediterranean region experience decreases in pigment contents and increases in carotenoids/chlorophyll (Car/Chl) ratio [60]. This change in Car/Chl ratios plays a key role in photosynthetic down-regulation, and is associated with variability in PRI [27,58]. Decreases in PRI and photosynthesis presented in this study thus indirectly suggested that changes in Car/Chl had a significant effect on photosynthetic down-regulation. Therefore, PRI detected the effect of the progressive drought on photosynthesis, consistent with many previous studies that have demonstrated that PRI is correlated with photosynthesis and Yield under water stress conditions [14,34].

Additionally, PRI was quite stable in the last three extreme drought level treatments (plants without water for 16–21 days), unlike the slight decrease of A, F_V/F_M, Yield, and R690/R630, reflecting the insensitivity of PRI to severe drought, at intensities where there is observable leaf fall. Previous leaf-level studies have reported that PRI was unable to assess the negative light use efficiency (LUE) of severely damaged plants [34]. Under severe stress conditions, evergreen leaves could retain zeaxanthin pigments to protect the photosystem from damage, which might contribute to such stability in PRI [61]. At canopy level, changes in structure, heterogeneity in irradiance, and differences in sun angles within the crown have hindered PRI interpretation and assessment of LUE [24]. At larger spatial scales, satellite-based (Moderate Resolution Imaging Spectroradiometer, MODIS) PRI has tracked ecosystem LUE, even during severe water limitation of summer for *Q. ilex* [62]. The normalized PRI by absorbed light detected the drought effect on gross primary production (GPP) in a deciduous forest and an evergreen broadleaf forest in France, but did not capture the reduction of GPP in a semi-arid grassland in Hungary [8]. Guarini et al. [36] demonstrated that MODIS-based PRI should be used with care under severe water stress, because the disturbances from canopy structure, illumination and viewing angles, and so forth, could increase the uncertainty of PRI in tracking LUE. These studies presented the complications of the applicability of PRI under severe drought conditions at different spatial scales, and other factors, such as soil backgrounds, vegetation functional types, atmospheric interference and instrument characteristics, can also complicate the applications of PRI in assessing LUE [24]. However, the strong correlations between PRI and A and ΦPSII (F_V/F_M and Yield) under enhanced drought levels demonstrate that PRI can be applied to detect the effect of continuously increased drought on photosynthesis for Mediterranean evergreen sclerophylls, which generally experience summer drought.

Interestingly, the reflectance ratio based on the red-edge region of the spectrum R690/R630 presented significant correlations with A, F_V/F_M, and Yield, and efficiently tracked the photosynthetic changes to enhanced drought levels (Figure 2b,d). Previous studies have shown reflectance ratios such as R685/R630 and R690/R630 are sensitive to changes in foliar F_V/F_M. Dobrowski et al. [31] used similar reflectance ratios to quantify the chlorophyll fluorescence (ChlF) emissions because of their superimposition at the red reflectance region, with a maximum emission in the near red-edge region of 690 and 740 nm. The reference band (e.g., R630 or R655) was chosen due to its insensitivity to ChlF emission and sensitivity to chlorophyll pigments [47]. These simple reflectance ratios have tracked the foliar ChlF under both diurnal natural, stress and recovery conditions [31,47,49]. The links between R690/R630 and ChlF emissions probably contribute to interpreting the relationships between R690/R630 and photosynthesis in this study. In addition, ChlF can increase under severely low quantum yields [63], however, continuous decreases in R690/R630 during extreme drought periods suggested that, apart from ChlF emission at 690 nm, other plant physiological functions also control the changes in R690/R630. The reabsorption of red ChlF (particularly at ChlF emission peak near 690 nm) by chlorophyll pigments can also affect the variability of R690/R630 [45]. Further, the low reflectance in the red-edge of the spectrum generally resulted from the high absorption of chlorophyll pigments. Zarco-Tejada et al. [49] showed the large effect of chlorophyll content on similar reflectance ratios such as R685/R630 and R680/R630. However, NDVI, which could indirectly indicate the chlorophyll pigment changes, was quite stable and did not track the photosynthetic activity during the study

period. The chlorophyll content thus probably had low effects on R690/R630 and its correlation with photosynthesis for this Mediterranean evergreen species.

Additionally, the down-regulation of maximum photochemical efficiency of PSII (F_V/F_M) is associated with changes of non-photochemical quenching (NPQ) under environmental stress [61,64,65]. The significant correlation of R690/R630 with F_V/F_M in this and previous diurnal studies [47,48] indicated that NPQ probably plays a key role in linking R690/R630 with changes in photosynthetic activity. Although PRI was also highly correlated with F_V/F_M, the rather constant PRI in the extreme drought conditions (the last three drought treatments) was decoupled with the strong depression of F_V/F_M. Such decoupling of PRI with LUE and NPQ was also found in early spring when Scots pine needles demonstrated large down-regulation due to the effect of severe stress [27]. In contrast, in our study, R690/R630 presented consistent changes with F_V/F_M, Yield and *A* even under extreme water stress conditions.

4.2. PRI and R690/R630 Tracked the Photosynthetic Recovery from Progressively Enhanced Drought Stresses

The CO_2 assimilation rates and ΦPSII of *Q. ilex* rapidly recovered to normal values that were similar with control (0-day drought level treatment) after five weeks of re-watering (Figure 3). The values of PRI and R690/R630 were increased to similar values after re-watering, indicating that both PRI and R690/R630 were also sensitive to the recovery of the plant. The significant correlations of differential PRI ($\Delta PRI_{recovery}$) and R690/R630 ($\Delta R690/R630_{recovery}$) with $\Delta A_{recovery}$, $\Delta F_V/F_{Mrecovery}$ and $\Delta Yield_{recovery}$ (Figure 5) illustrated their potential to monitor photosynthetic recovery response to drought stress.

PRI was originally defined to detect the variability of zeaxanthin changes at 531 nm [21,22]. However, it should be noted that 531 nm was the band associated with carotenoid pigment changes, including zeaxanthin, and also other carotenoid pigments such as lutein and neoxanthin [66]. These carotenoids both play key roles in energy dissipation of photosynthetic down- and up-regulation [67,68]. However, studies have demonstrated that constitutive long-term changes of PRI were greatly attributable to carotenoid pigment pool sizes [27,29,58,59]. Thus, the mechanism of PRI detecting photosynthetic recovery was probably due to the carotenoid pigments acting on the photochemical process. Also, during water stress and recovery, PRI was significantly correlated with carotenoid pigments in olive saplings [32].

In contrast with PRI, changes in R690/R630 were probably related with ChlF emissions but not with chlorophyll pigments for evergreen broadleaves in this study. ChlF is the energy of absorbed photosynthetically active radiation (APAR) that is lost during the first steps of photosynthesis which involves the emission of red to far-red light (ca. 660 to 800 nm) [39]. ChlF is therefore associated with the fraction of APAR and also with light use efficiency (LUE), giving the possibility of using R690/R630 to monitor photosynthetic recovery after experiencing different drought stresses. Additionally, ChlF is mainly emitted from PSII, so the recovery of photochemistry could increase the ChlF emission, particularly in red wavelengths at 690 nm, which is close to the absorption peak of the pigments of PSII [39,45]. Consequently, R690/R630 is a good indicator of photosynthetic recovery in response to progressive drought stress for evergreen leaves.

5. Conclusions and Final Remarks

This study makes progress in assessing mild to extreme drought stresses in Mediterranean evergreen species with the PRI and reflectance ratio R690/R630. Both PRI and R690/R630 were not only sensitive to progressive drought, but also to plant recovery, significantly tracking the photosynthetic response to enhanced drought levels, and also detecting the photosynthetic recovery after re-watering. Carotenoid/chlorophyll pigment ratios probably control the correlation between PRI and photosynthesis, and ChlF at 690 nm probably plays a role in the relationship of R690/R630 with photosynthesis. Both PRI and R690/R630 can be used for remotely monitoring the effect of drought on the carbon uptake and productivity of Mediterranean species.

Our work also promotes the possibility of parameterizing LUE models based on the PRI and the ratio R690/R630 for evergreen species. This is because of links between PRI is linked with short-term changes in xanthophyll pigments proportions and long-term shifts in pigment pools, and R690/R630 with chlorophyll content and fluorescence [69]. For other non-evergreen vegetation such as annual or deciduous plants, the potential uses of PRI and R690/R630 in detecting the progressive drought and recovery effects on photosynthetic activity should be further tested given their different physiological traits, but these results open a promising window for them too. The increasing use of hyperspectral spectroradiometers carried on unmanned aerial vehicles (UAVs) [70] and satellites (such as Metop and Sentinel series) provides the possibility of testing the LUE model using PRI and red-edge reflectance indices for multiple vegetation types and at different spatiotemporal scales.

Author Contributions: Josep Peñuelas, Catherine Preece and Iolanda Filella conceived and designed the experiments; Chao Zhang, Catherine Preece, Iolanda Filella and Gerard Farré-Armengol performed the experiments; Chao Zhang analyzed the data and wrote the initial draft and figures. All of the authors contributed to the discussion of the results and to the writing of the manuscript.

Conflicts of Interest: The authors declare no conflict of interest.

References

1. Hoerling, M.; Eischeid, J.; Perlwitz, J.; Quan, X.; Zhang, T.; Pegion, P. On the increased frequency of Mediterranean drought. *J. Clim.* **2012**, *25*, 2146–2161. [CrossRef]
2. Giorgi, F.; Lionello, P. Climate change projections for the Mediterranean region. *Glob. Planet. Chang.* **2008**, *63*, 90–104. [CrossRef]
3. Nicault, A.; Alleaume, S.; Brewer, S.; Carrer, M.; Nola, P.; Guiot, J. Mediterranean drought fluctuation during the last 500 years based on tree-ring data. *Clim. Dyn.* **2008**, *31*, 227–245. [CrossRef]
4. Peñuelas, J.; Sardans, J.; Filella, I.; Estiarte, M.; Llusià, J.; Ogaya, R.; Carnicer, J.; Bartrons, M.; Rivas-Ubach, A.; Grau, O.; et al. Assessment of the impacts of climate change on Mediterranean terrestrial ecosystems based on data from field experiments and long-term monitored field gradients in Catalonia. *Environ. Exp. Bot.* **2017**. [CrossRef]
5. Liu, D.; Llusia, J.; Ogaya, R.; Estiarte, M.; Llorens, L.; Yang, X.; Peñuelas, J. Physiological adjustments of a Mediterranean shrub to long-term experimental warming and drought treatments. *Plant Sci.* **2016**, *252*, 53–61. [CrossRef] [PubMed]
6. Granda, E.; Camarero, J.J.; Gimeno, T.E.; Martínez-Fernández, J.; Valladares, F. Intensity and timing of warming and drought differentially affect growth patterns of co-occurring Mediterranean tree species. *Eur. J. For. Res.* **2013**, *132*, 469–480. [CrossRef]
7. Liu, D.; Ogaya, R.; Barbeta, A.; Yang, X.; Peñuelas, J. Contrasting impacts of continuous moderate drought and episodic severe droughts on the aboveground-biomass increment and litterfall of three coexisting Mediterranean woody species. *Glob. Chang. Biol.* **2015**, *21*, 4196–4209. [CrossRef] [PubMed]
8. Vicca, S.; Balzarolo, M.; Filella, I.; Granier, A.; Herbst, M.; Knohl, A.; Longdoz, B.; Mund, M.; Nagy, Z.; Pintér, K.; et al. Remotely-sensed detection of effects of extreme droughts on gross primary production. *Sci. Rep.* **2016**, *6*, 1–13. [CrossRef] [PubMed]
9. Barbeta, A.; Ogaya, R.; Peñuelas, J. Dampening effects of long-term experimental drought on growth and mortality rates of a Holm oak forest. *Glob. Chang. Biol.* **2013**, *19*, 3133–3144. [CrossRef] [PubMed]
10. Iglesias, A.; Garrote, L.; Flores, F.; Moneo, M. Challenges to manage the risk of water scarcity and climate change in the Mediterranean. *Water Resour. Manag.* **2007**, *21*, 775–788. [CrossRef]
11. Lloret, F.; Siscart, D.; Dalmases, C. Canopy recovery after drought dieback in holm-oak Mediterranean forests of Catalonia (NE Spain). *Glob. Chang. Biol.* **2004**, *10*, 2092–2099. [CrossRef]
12. Turner, N.C. Sustainable production of crops and pastures under drought in a Mediterranean environment. *Ann. Appl. Biol.* **2004**, *144*, 139–147. [CrossRef]

13. Farquhar, G.D.; Sharkey, T.D. Stomatal conductance and photosynthesis. *Annu. Rev. Plant Physiol.* **1982**, *33*, 317–345. [CrossRef]

14. Peñuelas, J.; Filella, I.; Llusia, J.; Siscart, D.; Pinol, J. Comparative field study of spring and summer leaf gas exchange and photobiology of the mediterranean trees *Quercus ilex* and *Phillyrea latifolia*. *J. Exp. Bot.* **1998**, *49*, 229–238. [CrossRef]

15. Peña-Rojas, K.; Aranda, X.; Fleck, I. Stomatal limitation to CO_2 assimilation and down-regulation of photosynthesis in *Quercus ilex* resprouts in response to slowly imposed drought. *Tree Physiol.* **2004**, *24*, 813–822. [CrossRef] [PubMed]

16. Ogaya, R.; Llusià, J.; Barbeta, A.; Asensio, D.; Liu, D.; Alessio, G.A.; Peñuelas, J. Foliar CO_2 in a holm oak forest subjected to 15 years of climate change simulation. *Plant Sci.* **2014**, *226*, 101–107. [CrossRef] [PubMed]

17. De Rigo, D.; Caudullo, G. *Quercus ilex* in Europe: Distribution, habitat, usage and threats. In *European Atlas of Forest Tree Species*; European Union: Luxembourg, 2016; pp. 130–131.

18. Vaz, M.; Pereira, J.S.; Gazarini, L.C.; David, T.S.; David, J.S.; Rodrigues, A.; Maroco, J.; Chaves, M.M. Drought-induced photosynthetic inhibition and autumn recovery in two Mediterranean oak species (*Quercus ilex* and *Quercus suber*). *Tree Physiol.* **2010**, *30*, 946–956. [CrossRef] [PubMed]

19. Demmig-Adams, B.; Adams, W.W. The role of xanthophyll cycle carotenoids in the protection of photosynthesis. *Trends Plant Sci.* **1996**, *1*, 21–26. [CrossRef]

20. Adams, W.W.; Demmig-Adams, B. Carotenoid composition and down regulation of photosystem II in three conifer species during the winter. *Physiol. Plant.* **1994**, *92*, 451–458. [CrossRef]

21. Gamon, J.A.; Peñuelas, J.; Field, C. A narrow-waveband spectral index that tracks diurnal changes in photosunthetic efficiency. *Remote Sens. Environ.* **1992**, *41*, 35–44. [CrossRef]

22. Peñuelas, J.; Filella, I.; Gamon, J.A. Assessment of photosynthetic radiation use efficiency with spectral reflectance. *New Phytol.* **1995**, *131*, 291–296. [CrossRef]

23. Garbulsky, M.F.; Peñuelas, J.; Gamon, J.; Inoue, Y.; Filella, I. The photochemical reflectance index (PRI) and the remote sensing of leaf, canopy and ecosystem radiation use efficiencies. A review and meta-analysis. *Remote Sens. Environ.* **2011**, *115*, 281–297. [CrossRef]

24. Zhang, C.; Filella, I.; Garbulsky, M.; Peñuelas, J. Affecting factors and recent improvements of the photochemical reflectance index (PRI) for remotely sensing foliar, canopy and ecosystemic radiation-use efficiencies. *Remote Sens.* **2016**, *8*, 677. [CrossRef]

25. Peñuelas, J.; Garbulsky, M.F.; Filella, I.; Papp, T. Photochemical reflectance index (PRI) and remote sensing of plant CO_2 uptake. *New Phytol.* **2011**, *191*, 596–599. [CrossRef] [PubMed]

26. Garbulsky, M.F.; Peñuelas, J.; Papale, D.; Ardö, J.; Goulden, M.L.; Kiely, G.; Richardson, A.D.; Rotenberg, E.; Veenendaal, E.M.; Filella, I. Patterns and controls of the variability of radiation use efficiency and primary productivity across terrestrial ecosystems. *Glob. Ecol. Biogeogr.* **2010**, *19*, 253–267. [CrossRef]

27. Porcar-Castell, A.; Garcia-Plazaola, J.I.; Nichol, C.J.; Kolari, P.; Olascoaga, B.; Kuusinen, N.; Fernández-Marín, B.; Pulkkinen, M.; Juurola, E.; Nikinmaa, E. Physiology of the seasonal relationship between the photochemical reflectance index and photosynthetic light use efficiency. *Oecologia* **2012**, *170*, 313–323. [CrossRef] [PubMed]

28. Peñuelas, J.; Gamon, J.A.; Fredeen, A.L.; Merino, J.; Field, C.B. Reflectance indices associated with physiological changes in nitrogen- and water-limited sunflower leaves. *Remote Sens. Environ.* **1994**, *48*, 135–146. [CrossRef]

29. Wong, C.Y.S.; Gamon, J.A. Three causes of variation in the photochemical reflectance index (PRI) in evergreen conifers. *New Phytol.* **2015**, *206*, 187–195. [CrossRef] [PubMed]

30. Frank, H.A.; Cogdell, R.J. Carotenoids in photosynthesis. *Photochem. Photobiol.* **1996**, *63*, 257–264. [CrossRef] [PubMed]

31. Dobrowski, S.Z.; Pushnik, J.C.; Zarco-Tejada, P.J.; Ustin, S.L. Simple reflectance indices track heat and water stress-induced changes in steady-state chlorophyll fluorescence at the canopy scale. *Remote Sens. Environ.* **2005**, *97*, 403–414. [CrossRef]

32. Sun, P.; Wahbi, S.; Tsonev, T.; Haworth, M.; Liu, S.; Centritto, M. On the use of leaf spectral indices to assess water status and photosynthetic limitations in *Olea europaea* L. during water-stress and recovery. *PLoS ONE* **2014**, *9*, e105165. [CrossRef] [PubMed]

33. Moreno, A.; Maselli, F.; Gilabert, M.A.; Chiesi, M.; Martínez, B.; Seufert, G. Assessment of MODIS imagery to track light-use efficiency in a water-limited Mediterranean pine forest. *Remote Sens. Environ.* **2012**, *123*, 359–367. [CrossRef]

34. Peñuelas, J.; Llusia, J.; Pinol, J.; Filella, I.; Penuelas, J.; Llusia, J.; Pinol, J.; Filella, I. Photochemical reflectance index and leaf photosynthetic radiation-use-efficiency assessment in Mediterranean trees. *Int. J. Remote Sens.* **1997**, *18*, 2863–2868. [CrossRef]

35. Filella, I.; Amaro, T.; Araus, J.L.; Peñuelas, J. Relationship between photosynthetic radiation-use efficiency of barley canopies and the photochemical reflectance index (PRI). *Physiol. Plant.* **1996**, *96*, 211–216. [CrossRef]

36. Guarini, R.; Nichol, C.; Clement, R.; Loizzo, R.; Grace, J.; Borghetti, M. The utility of MODIS-sPRI for investigating the photosynthetic light-use efficiency in a Mediterranean deciduous forest. *Int. J. Remote Sens.* **2014**, *35*, 6157–6172. [CrossRef]

37. Krause, G.; Weis, E. Chlorophyll fluorescence and photosynthesis: The basics. *Annu. Rev. Plant Physiol. Plant Mol. Biol.* **1991**, *42*, 313–349. [CrossRef]

38. Lichtenthaler, H.K.; Miehé, J.A. Fluorescence imaging as a diagnostic tool for plant stress. *Trends Plant Sci.* **1997**, *2*, 316–320. [CrossRef]

39. Porcar-Castell, A.; Tyystjärvi, E.; Atherton, J.; Van Der Tol, C.; Flexas, J.; Pfündel, E.E.; Moreno, J.; Frankenberg, C.; Berry, J.A. Linking chlorophyll a fluorescence to photosynthesis for remote sensing applications: Mechanisms and challenges. *J. Exp. Bot.* **2014**, *65*, 4065–4095. [CrossRef] [PubMed]

40. Ač, A.; Malenovský, Z.; Olejníčková, J.; Gallé, A.; Rascher, U.; Mohammed, G. Meta-analysis assessing potential of steady-state chlorophyll fluorescence for remote sensing detection of plant water, temperature and nitrogen stress. *Remote Sens. Environ.* **2015**, *168*, 420–436. [CrossRef]

41. Guanter, L.; Zhang, Y.; Jung, M.; Joiner, J.; Voigt, M.; Berry, J.A.; Frankenberg, C.; Huete, A.R.; Zarco-Tejada, P.; Lee, J.-E.; et al. Global and time-resolved monitoring of crop photosynthesis with chlorophyll fluorescence. *Proc. Natl. Acad. Sci. USA* **2014**, *111*, E1327–E1333. [CrossRef] [PubMed]

42. Carter, G.A.; Jones, J.H.; Mitchell, R.J.; Brewer, C.H. Detection of solar-excited chlorophyll a fluorescence and leaf photosynthetic capacity using a Fraunhofer Line Radiometer. *Remote Sens. Environ.* **1996**, *55*, 89–92. [CrossRef]

43. Zarco-Tejada, P.J.; González-Dugo, M.V.; Fereres, E. Seasonal stability of chlorophyll fluorescence quantified from airborne hyperspectral imagery as an indicator of net photosynthesis in the context of precision agriculture. *Remote Sens. Environ.* **2016**, *179*, 89–103. [CrossRef]

44. Freedman, A.; Cavender-Bares, J.; Kebabian, P.L.; Bhaskar, R.; Scott, H.; Bazzaz, F.A. Remote sensing of solar-excited plant fluorescence as a measure of photosynthetic rate. *Photosynthetica* **2002**, *40*, 127–132. [CrossRef]

45. Buschmann, C.; Lichtenthaler, H.K. Principles and characteristics of multi-colour fluorescence imaging of plants. *J. Plant Physiol.* **1998**, *152*, 297–314. [CrossRef]

46. Meroni, M.; Rossini, M.; Guanter, L.; Alonso, L.; Rascher, U.; Colombo, R.; Moreno, J. Remote sensing of solar-induced chlorophyll fluorescence: Review of methods and applications. *Remote Sens. Environ.* **2009**, *113*, 2037–2051. [CrossRef]

47. Zarco-Tejada, P.J.; Miller, J.R.; Mohammed, G.H.; Nolan, T.L. Chlorophyll fluoresence effects on vegetation apparent reflectanc: I. Leaf-level measurements and model simulation. *Remote Sens. Environ.* **2000**, *74*, 582–592. [CrossRef]

48. Zarco-Tejada, P.J.; Miller, J.R.; Mohammed, G.H.; Noland, T.L.; Sampson, P.H. Chlorophyll fluorescence effects on vegetation apparent reflectance: II. Laboratory and Airborne canopy-level measurements with hyperspectral data. *Remote Sens. Environ.* **2000**, *74*, 596–608. [CrossRef]

49. Zarco-Tejada, P.J.; Berni, J.A.J.; Suárez, L.; Sepulcre-Cantó, G.; Morales, F.; Miller, J.R. Imaging chlorophyll fluorescence with an airborne narrow-band multispectral camera for vegetation stress detection. *Remote Sens. Environ.* **2009**, *113*, 1262–1275. [CrossRef]

50. Ač, A.; Olejníčková, J.; Mishra, K.B.; Malenovský, Z.; Hanuš, J.; Trtílek, M.; Nedbal, L.; Marek, M.V. Towards remote sensing of vegetation processes. In Proceedings of the Workshop Sensing a Changing World 2008, Wageningen, The Netherlands, 19–21 Novemebr 2008; pp. 19–23.

51. Ač, A.; Malenovský, Z.; Hanuš, J.; Tomášková, I.; Urban, O.; Marek, M.V. Near-distance imaging spectroscopy investigating chlorophyll fluorescence and photosynthetic activity of grassland in the daily course. *Funct. Plant Biol.* **2009**, *36*, 1006–1015. [CrossRef]

52. Furuuchi, H.; Jenkins, M.W.; Senock, R.S.; Houpis, J.L.J.; Pushnik, J.C. Estimating plant crown transpiration and water use efficiency by vegetative reflectance indices associated with chlorophyll fluorescence. *Open J. Ecol.* **2013**, *3*, 122–132. [CrossRef]

53. Ni, Z.Y.; Liu, Z.G.; Li, Z.L.; Nerry, F.; Huo, H.Y.; Li, X.W. Estimation of solar-induced fluorescence using the canopy reflectance index. *Int. J. Remote Sens.* **2015**, *36*, 5239–5256. [CrossRef]

54. Panigada, C.; Rossini, M.; Meroni, M.; Cilia, C.; Busetto, L.; Amaducci, S.; Boschetti, M.; Cogliati, S.; Picchi, V.; Pinto, F.; et al. Fluorescence, PRI and canopy temperature for water stress detection in cereal crops. *Int. J. Appl. Earth Obs. Geoinf.* **2014**, *30*, 167–178. [CrossRef]

55. Zarco-Tejada, P.J.; González-Dugo, V.; Williams, L.E.; Suárez, L.; Berni, J.A.J.; Goldhamer, D.; Fereres, E. A PRI-based water stress index combining structural and chlorophyll effects: Assessment using diurnal narrow-band airborne imagery and the CWSI thermal index. *Remote Sens. Environ.* **2013**, *138*, 38–50. [CrossRef]

56. Rossini, M.; Fava, F.; Cogliati, S.; Meroni, M.; Marchesi, A.; Panigada, C.; Giardino, C.; Busetto, L.; Migliavacca, M.; Amaducci, S.; et al. Assessing canopy PRI from airborne imagery to map water stress in maize. *ISPRS J. Photogramm. Remote Sens.* **2013**, *86*, 168–177. [CrossRef]

57. Genty, B.; Briantais, J.-M.; Baker, N.R. The relationship between the quantum yield of photosynthetic electron transport and quenching of chlorophyll fluorescence. *Biochim. Biophys. Acta Gen. Subj.* **1989**, *990*, 87–92. [CrossRef]

58. Filella, I.; Porcar-Castell, A.; Munné-Bosch, S.; Bäck, J.; Garbulsky, M.F.; Peñuelas, J. PRI assessment of long-term changes in carotenoids/chlorophyll ratio and short-term changes in de-epoxidation state of the xanthophyll cycle. *Int. J. Remote Sens.* **2009**, *30*, 4443–4455. [CrossRef]

59. Gamon, J.A.; Berry, J.A. Facultative and constitutive pigment effects on the photochemical reflectance index (PRI) in sun and shade conifer needles. *Isr. J. Plant Sci.* **2012**, *60*, 85–95. [CrossRef]

60. Baquedano, F.J.; Castillo, F.J. Comparative ecophysiological effects of drought on seedlings of the Mediterranean water-saver *Pinus halepensis* and water-spenders *Quercus coccifera* and *Quercus ilex*. *Trees Struct. Funct.* **2006**, *20*, 689–700. [CrossRef]

61. Demmig-Adams, B.; Adams, W.W. Photoprotection in an ecological context: The remarkable complexity of thermal energy dissipation. *New Phytol.* **2006**, *172*, 11–21. [CrossRef] [PubMed]

62. Goerner, A.; Reichstein, M.; Rambal, S. Tracking seasonal drought effects on ecosystem light use efficiency with satellite-based PRI in a Mediterranean forest. *Remote Sens. Environ.* **2009**, *113*, 1101–1111. [CrossRef]

63. Van Der Tol, C.; Berry, J.A.; Campbell, P.K.E.; Rascher, U. Models of fluorescence and photosynthesis for interpreting measurements of solar-induced chlorophyll fluorescence. *J. Geophys. Res. Biogeosci.* **2014**, *119*, 2312–2327. [CrossRef] [PubMed]

64. Porcar-Castell, A. A high-resolution portrait of the annual dynamics of photochemical and non-photochemical quenching in needles of *Pinus sylvestris*. *Physiol. Plant.* **2011**, *143*, 139–153. [CrossRef] [PubMed]

65. Verhoeven, A. Sustained energy dissipation in winter evergreens. *New Phytol.* **2014**, *201*, 57–65. [CrossRef]

66. Gitelson, A.A.; Zur, Y.; Chivkunova, O.B.; Merzlyak, M.N. Assessing carotenoid content in plant leaves with reflectance spectroscopy. *Photochem. Photobiol.* **2002**, *75*, 272–281. [CrossRef]

67. Ruban, A.V.; Berera, R.; Ilioaia, C.; van Stokkum, I.H.M.; Kennis, J.T.M.; Pascal, A.A.; van Amerongen, H.; Robert, B.; Horton, P.; van Grondelle, R. Identification of a mechanism of photoprotective energy dissipation in higher plants. *Nature* **2007**, *450*, 575–578. [CrossRef] [PubMed]

68. Jahns, P.; Holzwarth, A.R. The role of the xanthophyll cycle and of lutein in photoprotection of photosystem II. *Biochim. Biophys. Acta Bioenerg.* **2012**, *1817*, 182–193. [CrossRef] [PubMed]

69. Gamon, J.A. Reviews and Syntheses: Optical sampling of the flux tower footprint. *Biogeosciences* **2015**, *12*, 4509–4523. [CrossRef]

70. Gago, J.; Douthe, C.; Coopman, R.E.; Gallego, P.P.; Ribas-Carbo, M.; Flexas, J.; Escalona, J.; Medrano, H. UAVs challenge to assess water stress for sustainable agriculture. *Agric. Water Manag.* **2015**, *153*, 9–19. [CrossRef]